The ω-absorption line distribution function for rank correlated SLW model prediction of radiative transfer in non-uniform gases

Frédéric André, Vladimir Solovjov, Brent Webb

THE ω-ABSORPTION LINE DISTRIBUTION FUNCTION FOR RANK CORRELATED SLW MODEL PREDICTION OF RADIATIVE TRANSFER IN NON-UNIFORM GASES

Frédéric André[*,§], Vladimir P. Solovjov[**], Brent W. Webb[**]

[*]Univ Lyon, CNRS, INSA-Lyon, Université Claude Bernard Lyon 1, CETHIL UMR 5008, F-69621Villeurbanne, France

[**]Department of Mechanical Engineering, Brigham Young University, Provo, UT 84602, USA

[§]Correspondence author. Fax: +33 4 7243 8816 Email: frederic.andre@insa-lyon.fr

ABSTRACT

Unlike previous global methods, the recently developed Rank Correlated Spectral Line Weighted-sum-of-gray-gases (RC-SLW) model does not require specification of a reference gas thermodynamic state from which all other states are corrected using a correlated spectrum assumption. However, the RC-SLW approach still requires specification of an arbitrary blackbody source temperature to generate the Absorption Line Blackbody Distribution Function (ALBDF) used in construction of the spectral model. This paper reports on the development of a universal RC-SLW model that eliminates the need for the specification of a blackbody source temperature. The approach replaces the ALBDF with a new spectral distribution function, herein termed the ω-Absorption Line Distribution Function (ω-ALDF), and is based on a new spectral weighting function instead of the Planck blackbody distribution function. The ω-ALDF presented here depends only on the local gas thermodynamic state, and does not involve the blackbody source temperature used in the ALBDF. The new weighting function is determined using the well-established ALBDF, avoiding the need to generate a radically new distribution function database from the detailed gas absorption cross-section data. The ω-ALDF based RC-SLW model thus requires no user-specified parameters (no reference thermodynamic state and no blackbody source temperature). Further, only minor modification of the conventional RC-SLW model is needed to implement the new approach. Development of this new distribution function is only possible within the theoretical framework of the Rank Correlated SLW model. This work presents the theoretical development of the ω-ALDF, and demonstrates the use and accuracy of this new universal RC-SLW model.

INTRODUCTION

Spatial Averaging (SA) techniques are used widely in gas radiation modeling for the treatment of non-uniform situations. In fact, SA methods allow the transformation of complicated non-uniform problems that cannot be solved easily in the general case, into equivalent uniform problems for which models exist. Examples of non-uniform methods based on SA techniques encountered frequently in gas radiation modeling are the Curtis-Godson or Lindquist-Simmons approximations, in the context of Statistical Narrow Band models [Young 2013] or, in a generalized form, in the full spectrum SLMB method [Andre 2008]. In these cases, spatial averaging is performed along a line-of-sight. In other global approaches, such as SLW, ADF, or FSK methods, spatial averaging is performed inside a gaseous volume and is usually applied to define reference states for these methods [Denison 1993, Pierrot 1999, Modest 2003].

In the RC-SLW/RC-FSK models [Solovjov 2017, Solovjov 2018a] for predicting radiative transfer in high-temperature gases, there is no need to define any kind of reference state of the gas. However, in the existing RC-SLW model's formulation a blackbody source temperature is still required to construct the model. This source temperature provides the definition of a spectral measure on the wavenumber axis required to evaluate distribution functions of absorption coefficients or absorption cross-sections, called the Absorption Line Blackbody Distribution Function (ALBDF) in SLW modeling. The ALBDF is the fundamental quantity in the SLW model, used both to associate spectra in distinct states through the so-called correlation assumption and also, from a practical perspective, to generate all the required model parameters, *i.e.*, the local absorption cross-sections and corresponding weights.

The ALBDF is defined as the fraction of blackbody intensity at a temperature T_b calculated over all wavenumbers where the spectral cross-section is below a prescribed value. The ALBDF thus requires a temperature, T_b, on which the Planck spectral blackbody distribution function is based, to evaluate these blackbody intensities. All global methods require a spectral weighting function to treat more than one thermodynamic state - a spectral measure required to define the probability to encounter a given value of absorption coefficient. In all current FSCK and SLW global models, that spectral weighting function has been the Planck blackbody spectral distribution, usually generated at

a specified reference temperature (*i.e.*, reference state) $T_b = T_{ref}$. However, it was demonstrated in [Andre 2017] that, in theory, any strictly positive and normalized function of wavenumber $\omega(\eta)$ can be used to define distribution functions of either the *k* (absorption coefficient) or *C* (absorption cross-section) variables. The aim of the present work is to provide a method to generate such a function $\omega(\eta)$ in place of the Planck spectral blackbody intensity $I_b(\eta)$ used in the conventional RC-SLW model. Indeed, such an approach was presented by Maurente [2017], although it still required a user-defined parameter ($\eta_{\max}$), and necessitated the generation of an entirely new spectral database. The work developed here leads to a version of the RC-SLW method that does not require any reference to a rather arbitrarily chosen blackbody source temperature. The presently proposed version of the RC-SLW method is thus free from any user-specified parameter (either gas reference state or blackbody source temperature). Further, the model presented here utilizes existing spectral databases. The model is, consequently, the first full spectrum method of this kind in the gas radiation modeling literature. The theoretical development of the current approach to generate a new spectral function $\omega(\eta)$ uses as its basis the RC-SLW model formulation.

DERIVATION OF THE ω-ALDF MODEL

Choice of the ω function The objective of this theoretical development is to define a function $\omega(\eta)$ of wavenumbers that has the following properties:

$$\begin{gathered} \omega(\eta) > 0 \\ \int_0^{+\infty} \omega(\eta)\ d\eta = 1 \end{gathered} \tag{1}$$

(Note that this function was denoted $\mu(\eta)$ in [Andre 2017] to represent a spectral measure on the real line. Here, the notation $\omega(\eta)$ has been chosen to represent a spectral weighting scheme. However, the two notations are mathematically equivalent.) The normalization constraint set by the second relationship in Eq. (1) is not strictly mandatory, but it ensures that the integral of the function $\omega(\eta)$ over all possible values of wavenumbers is bounded. The problem is formulated as follows.

Consider a non-uniform volume of gas V. Inside a small volume element dV, the temperature of the gas is $T(dV)$ and the molar fraction of absorbing species is $Y(dV)$. The spectral absorption coefficient of the gas in dV is $k_\eta\left[Y(dV),T(dV)\right] = Y(dV)\cdot C_\eta\left[Y(dV),T(dV)\right]$. Notice that in order to abridge the notations, the spectral variable C_η considered here is defined as the product of

the true spectral absorption cross-section and the molar density. The corresponding Planck mean absorption coefficient, which characterizes the emission by the gas at the local thermophysical state of the gas in dV, is:

$$k_P(dV) = Y(dV)\, C_P(dV)$$

$$C_P(dV) = \int_0^{+\infty} C_\eta\left[Y(dV), T(dV)\right] \frac{I_{b\eta}\left[T(dV)\right]}{I_b\left[T(dV)\right]}\, d\eta \tag{2}$$

Over the volume V, one can evaluate a volume-integrated spectral absorption cross-section as:

$$\bar{C}_\eta = \frac{1}{\bar{Y}} \int_V Y(dV)\, C_\eta\left[Y(dV), T(dV)\right] dV, \quad \bar{Y} = \int_V Y(dV)\, dV \tag{3}$$

It is proposed to define the spectral weighting function $\omega(\eta)$ as the function that, when applied to the volume-integrated absorption cross-section defined by Eq. (3), provides the same value of Planck mean as its exact counterpart, calculated as the volume integral of all local Planck means. In other words, one may define $\omega(\eta)$ as solution of the following equality:

$$\int_0^{+\infty} \bar{C}_\eta\, \omega(\eta)\, d\eta = \frac{1}{\bar{Y}} \int_V Y(dV)\, C_P(dV)\, dV \tag{4}$$

Other choices of $\omega(\eta)$ functions are possible, but the present one has reasonable physical basis and, as shown later in this paper, provides limiting cases that comply with some existing methods.

In order to solve this relationship for the unknown function $\omega(\eta)$, Eq. (2) is first rewritten as:

$$C_P(dV) = \int_0^{+\infty} \bar{C}_\eta \frac{I_{b\eta}\left[T(dV)\right]}{I_b\left[T(dV)\right]}\, d\eta + \int_0^{+\infty} \left\{C_\eta\left[Y(dV), T(dV)\right] - \bar{C}_\eta\right\} \frac{I_{b\eta}\left[T(dV)\right]}{I_b\left[T(dV)\right]}\, d\eta \tag{5}$$

The second integral on the right-hand side can be simplified as:

$$\int_0^{+\infty} \left\{C_\eta\left[Y(dV), T(dV)\right] - \bar{C}_\eta\right\} \frac{I_{b\eta}\left[T(dV)\right]}{I_b\left[T(dV)\right]}\, d\eta \approx \frac{1}{\eta^*(\varepsilon)} \int_0^{+\infty} \left\{C_\eta\left[Y(dV), T(dV)\right] - \bar{C}_\eta\right\} d\eta \tag{6}$$

where $\eta^*(\varepsilon)$ is defined through the relationship

$$\underset{T^* \in T(dV)}{Max} \left\{ \eta(\varepsilon) \text{ such that: } \int_0^{\eta(\varepsilon)} \frac{I_{b\eta}(T^*)}{I_b(T^*)}\, d\eta = 1 - \varepsilon \right\} \tag{7}$$

in which $\varepsilon \approx 0$ is a small, positive real number that defines the limits of acceptable accuracy in the assumption. The theoretical justification for the approximation of Eq. (6) is included in Appendix A.

Although the justification presents confirmation of the plausibility of the assumption in Eq. (6), the real test of its validity and the model on which it is based will be the comparison of model predictions with rigorous line-by-line benchmark predictions.

Equations (5) and (6) can now be inserted on the right-hand side of Eq. (4) to yield:

$$\begin{aligned}\frac{1}{\overline{\overline{Y}}}\int_V Y(dV)\,C_P(dV)\,dV \approx \frac{1}{\overline{\overline{Y}}}\int_V Y(dV)\left\{\int_0^{+\infty}\bar{C}_\eta\,\frac{I_{b\eta}\left[T(dV)\right]}{I_b\left[T(dV)\right]}\,d\eta\right\}dV \\ +\frac{1}{\overline{\overline{Y}}}\int_V Y(dV)\left\{\frac{1}{\eta^*(\varepsilon)}\int_0^{+\infty}\left\{C_\eta\left[Y(dV),T(dV)\right]-\bar{C}_\eta\right\}d\eta\right\}dV\end{aligned} \tag{8}$$

The second integral is obviously identically zero, by definition of the volume-integrated spectral absorption cross-section, Eq. (3). This allows one to write:

$$\frac{1}{\overline{\overline{Y}}}\cdot\int_V Y(dV)\,C_P(dV)\,dV = \frac{1}{\overline{\overline{Y}}}\int_V Y(dV)\left\{\int_0^{+\infty}\bar{C}_\eta\,\frac{I_{b\eta}\left[T(dV)\right]}{I_b\left[T(dV)\right]}\,d\eta\right\}dV \tag{9}$$

Eventually, the integrals over the volume and the wavenumbers can be exchanged to give:

$$\frac{1}{\overline{\overline{Y}}}\cdot\int_V Y(dV)\,C_P(dV)\,dV = \int_0^{+\infty}\bar{C}_\eta\left\{\frac{1}{\overline{\overline{Y}}}\int_V Y(dV)\,\frac{I_{b\eta}\left[T(dV)\right]}{I_b\left[T(dV)\right]}dV\right\}d\eta \tag{10}$$

Comparing Eqs. (4) and (10) provides, after identification, the following solution for $\omega(\eta)$:

$$\omega(\eta) = \frac{1}{\overline{\overline{Y}}}\int_V Y(dV)\,\frac{I_{b\eta}\left[T(dV)\right]}{I_b\left[T(dV)\right]}\,dV \tag{11}$$

This relationship can be rewritten in the following form, where δ is the Dirac Delta function:

$$\begin{aligned}\omega(\eta) &= \int_0^{+\infty} f(T)\,\frac{I_{b\eta}(T)}{I_b(T)}\,dT \\ f(T) &= \frac{1}{\overline{\overline{Y}}}\int_V Y(dV)\,\delta\left[T-T(dV)\right]dV\end{aligned} \tag{12}$$

The utility of this alternative formulation will be made more clear in the following section. From its definition Eq. (12), the function *f* multiplied by a small increment *dT* can be interpreted as the fraction of the gaseous volume occupied by the absorbing/emitting molecules for which the temperature of the gas lies in the interval [*T*, *T*+*dT*].

Definition of the ω-ALDF The function $\omega(\eta)$ derived in the foregoing section follows the constraints set by Eq. (1), and can thus be used as a weighting function on the wavenumber axis (in place of the Planck blackbody distribution function used in the ALBDF on which all SLW models are based). Following the theoretical developments detailed in [Andre 2017], one can thus, for any state of the gas for which the spectral values of the absorption coefficient are represented by variable $C_\eta = C_\eta(\phi)$, define a distribution function of absorption cross-sections as:

$$F_\omega(C,\phi) = \int_0^{+\infty} H\left[C - C_\eta(\phi)\right] \omega(\eta)\, d\eta \tag{13}$$

where H is the Heaviside step function and ϕ is a thermodynamic state vector that encompasses all the parameters (temperature, species concentrations, pressure) required to describe the thermophysical state of the gas. Note that Eq. (13) is similar both conceptually and mathematically to the definition of the ALBDF, but the Planck spectral blackbody intensity is replaced by the spectral distribution $\omega(\eta)$. The probability distribution of absorption cross-sections set by Eq. (13) is thus defined as the fraction of the function $\omega(\eta)$ over the set of wavenumbers for which $C > C_\eta(\phi)$. $F_\omega(C,\phi)$ is called the ω- Absorption Line Distribution Function (ω-ALDF), distinguished from the Absorption Line Blackbody Distribution Function (ALBDF) based on the Planck blackbody distribution. This new spectral function $\omega(\eta)$ *i*) depends only on the local state of the gas through the spectral variable $C_\eta = C_\eta(\phi)$, and *ii*) can be evaluated easily using the ALBDF together with Eq. (13), yielding directly (using an exchange of the two integrals with respect to temperature and wavenumbers involved in the definition):

$$F_\omega(C,\phi) = \int_0^{+\infty} f(T)\, F_b(C,\phi,T_b = T)\, dT \tag{14}$$

Here, each ALBDF $F_b(C,\phi,T_b = T)$ is the absorption line blackbody distribution function of C at the blackbody weighting temperature $T_b = T$, which can be different from the local temperature of the gas. As can be seen in Eq. (14), the ω-ALDF is not associated with any single value of temperature specified *a priori*, but is defined as a mixture (in the statistical sense) of distribution functions. Equation (14) allows the generation of values of the ω-ALDF directly from existing ALBDF databases, avoiding the need to generate a new spectral distribution database.

RESULTS AND DISCUSSION

Application of the ω-ALDF model within the framework of the RC-SLW approach Adaptation of the RC-SLW method to the framework of the ω-ALDF model requires only minor changes during the first steps of the construction of the model parameters from ALBDF look-up tables. In this section, a review of the method used in the conventional (ALBDF-based) RC-SLW approach is presented which generates local values of cross-sections from which both gray gas absorption coefficients and weights can be derived. The description is drawn principally from [Webb 2019, section 5.2.3], where additional details on the RC-SLW method can be found. Then, a description of how the method can be adapted for use with the ω-ALDF introduced here is presented. Throughout this section, the notations $X_i,\ i=1,..,N$ and $w_i,\ i=1,..,N$ will be used to represent the nodes and weights of a numerical quadrature of order *N* over the interval $[0,1]$.

One can consider an elementary volume *dV*, and the objective is to evaluate the RC-SLW model coefficients for the gas in *dV*, *i.e.*, local values of gray gas absorption cross-sections $C_i(dV)$ and their corresponding weights $a_i(dV)=F_b\left[\tilde{C}_{i+1}(dV),\phi(dV),T(dV)\right]-F_b\left[\tilde{C}_i(dV),\phi(dV),T(dV)\right]$ where $\tilde{C}_i(dV)$ are called supplemental cross-sections [Webb 2019].

In the original formulation of the RC-SLW method [Solovjov 2017, Webb 2019], local gray gas absorption coefficients are obtained as solutions of the following implicit equation which arises directly from the so-called correlation assumption:

$$F_b\left[C_i(dV),\phi(dV),T_b=T_{ave}\right]=X_i \tag{15}$$

Similarly, supplemental cross-sections are defined implicitly as:

$$F_b\left[\tilde{C}_i(dV),\phi(dV),T_b=T_{ave}\right]=\sum_{j=1}^{i-1}w_j \tag{16}$$

In Eqs. (15) and (16), T_{ave} is the average gas temperature of the gas in the volume *V* defined as:

$$T_{ave}=\frac{1}{V}\int_V T(dV)\,dV \tag{17}$$

One can notice that the implicit equations used to define the original RC-SLW model parameters depend explicitly on the mean temperature in the volume *V*, T_{ave}, which explains the dependence (even

if it is relatively weak for some problems in RC methods) of the solutions of the radiative transfer problems on the particular and arbitrary choice of blackbody source temperature T_b.

Application of the ω-ALDF method within the framework of the conventional RC-SLW (or its equivalent RC-FSK) method requires solving similar implicit equations by simply replacing the ALBDF $F_b\left[C(dV),\phi(dV),T_b=T_{ave}\right]$ in Eqs. (15) and (16) by the new spectral distribution function ω-ALDF $F_\omega\left[C(dV),\phi(dV)\right]$. This yields the following set of relationships to define gray gas absorption cross-sections:

$$F_\omega\left[C_i(dV),\phi(dV)\right]=\int_0^{+\infty} f(T)\,F_b\left[C_i(dV),\phi(dV),T\right]dT=X_i \tag{18}$$

Similarly, supplemental cross-sections are defined implicitly as:

$$F_\omega\left[\tilde{C}_i(dV),\phi(dV)\right]=\int_0^{+\infty} f(T)\,F_b\left[\tilde{C}_i(dV),\phi(dV),T\right]dT=\sum_{j=1}^{i-1} w_j \tag{19}$$

Using the ω-ALDF method, the explicit dependence of the solution of the RTE on the blackbody source temperature disappears. Indeed, implicit equations Eqs. (18) and (19) involve only local values of temperature inside each elementary volume *dV*, and do not refer to any pre-specified blackbody source temperature T_b as required by the ALBDF-based RC-SLW method in Eqs. (15) and (16).

In practice, instead of solving Eqs. (18) and (19) directly, ALBDF look-up tables may first be converted into tables of ω-ALDF by application of Eq. (14), following which the same computer routines used in the conventional RC-SLW model are employed in the radiative transfer solution. Using this method, the increase in computational cost related to application of ω-ALDFs is small, and only minor changes in existing codes for the RC-SLW method are needed. (Indeed, these changes concern only the calculation of ω-ALDFs from ALBDF look-up tables).

Example calculations

To demonstrate the implementation of the ω-ALDF-based RC-SLW method several example problems are considered treating a breath of radiative transfer problems. Consider a plane layer geometry in which gas is confined between two infinite black walls at the same temperature as the gas at $x = 0$ (left wall) and $x = L$ (right wall). In this study, the radiative transfer equation is solved using the multilayer semi-analytical solution method proposed by Solovjov and Webb [2008]. Six test cases are considered in this section, and in all cases the predicted local radiative flux divergence

for the ω-ALDF-based RC-SLW model and the ALBDF based RC-SLW model are compared against rigorous line-by-line benchmark solutions of the RTE. For the generation of the SLW model parameters, ALBDF look-up tables described in Pearson [2014] and freely available at http://albdf.byu.edu were used. As the objective of the present work is to the assess the notion of the ω-ALDF for radiative transfer calculations, no optimization of the number of gray gases was made, and 128 gray gases obtained by inversion of a Gauss-Legendre quadrature were used for all predictions. This high number of gray gases can be considered with reasonable confidence as the limit of the RC-SLW method for an infinite number of gray gases. This allows the evaluation solely of the concept of the ω-ALDF approach developed here, without any possible influence of the choice of the quadrature scheme (type of quadrature and order) on the quality of the solution. The two RC-SLW methods considered (ALBDF and ω-ALDF) in the following test cases use the same number of gray gases.

Cases 1 Case 1 considers a single absorbing gas (H_2O) diluted in nitrogen at atmospheric pressure. The temperature and water vapor profiles cases are given as:

$$T(x) = T_{\min} + \Delta T \sin(\pi x/L) \tag{20a}$$

$$Y_H(x) = Y_{H,\min} + \Delta Y_H \sin(\pi x/L) \tag{20b}$$

The temperature difference for this example is ΔT = 1500 K, and the H_2O concentration is uniform, $\Delta Y_H = 0$. The minimum temperature and H_2O concentration are, respectively, $T_{\min}$ = 500 K and $Y_{H,\min}$ = 0.3. The predicted local radiative flux divergence and local error (local absolute difference divided by the maximum value of flux divergence over the profile) relative to the line-by-line solution are shown in Fig. 1.

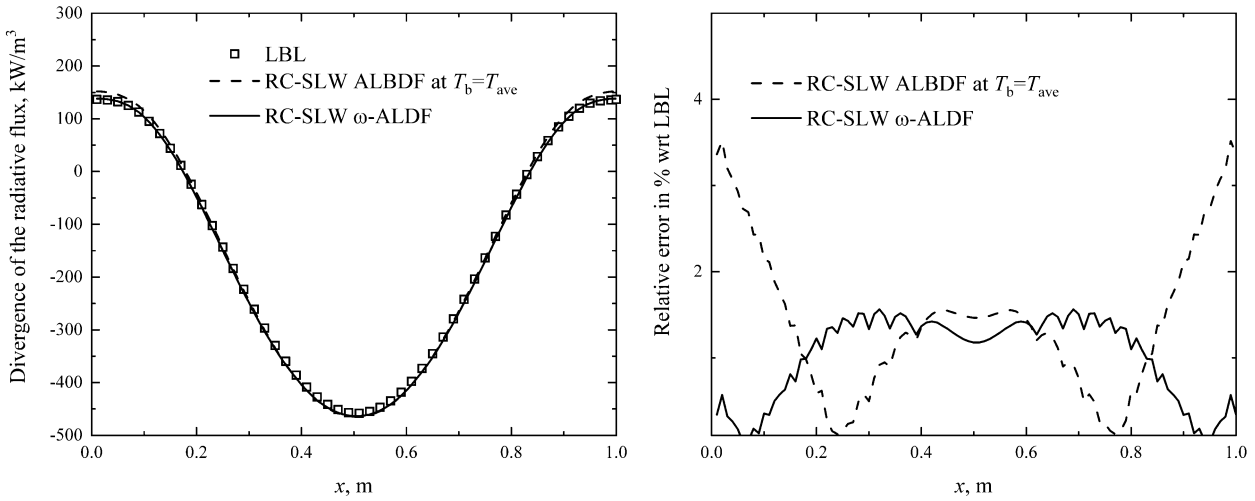

237

238 **Figure 1.** Single gas (H_2O) Case 1 (ΔT = 1500 K, ΔY_H = 0.0). Left: divergence of the radiative
239 flux. Right: relative error with respect to reference LBL calculations.

240 The LBL calculation is shown as square symbols, the corresponding RC-SLW model prediction based
241 on the ALBDF weighting function defined in terms of the blackbody source at the average
242 temperature of the gaseous medium is shown as a dashed line, and the RC-SLW model based on the
243 ω-ALDF model where the $\omega(\eta)$ function is obtained by application of Eq. (12) and the
244 corresponding distribution function using Eq. (14) is shown as a solid line. In this test case, the two
245 versions of the RC-SLW method are seen to provide high accuracy, with errors compared to the LBL
246 solution lower than 3.5%. Near the walls, the use of the ω-ALDF provides more accurate results than
247 the ALBDF evaluated at a blackbody source temperature T_b equal to the volume-averaged
248 temperature T_{ave}.

249 **Case 2** Case 2 is identical to Case 1 with the exception that the H_2O concentration varies spatially,
250 with maximum variation in H_2O mole fraction of $\Delta Y_H = 0.2$. This case thus explores a combined
251 non-isothermal, non-homogeneous example. Predictions are shown in Fig. 2.

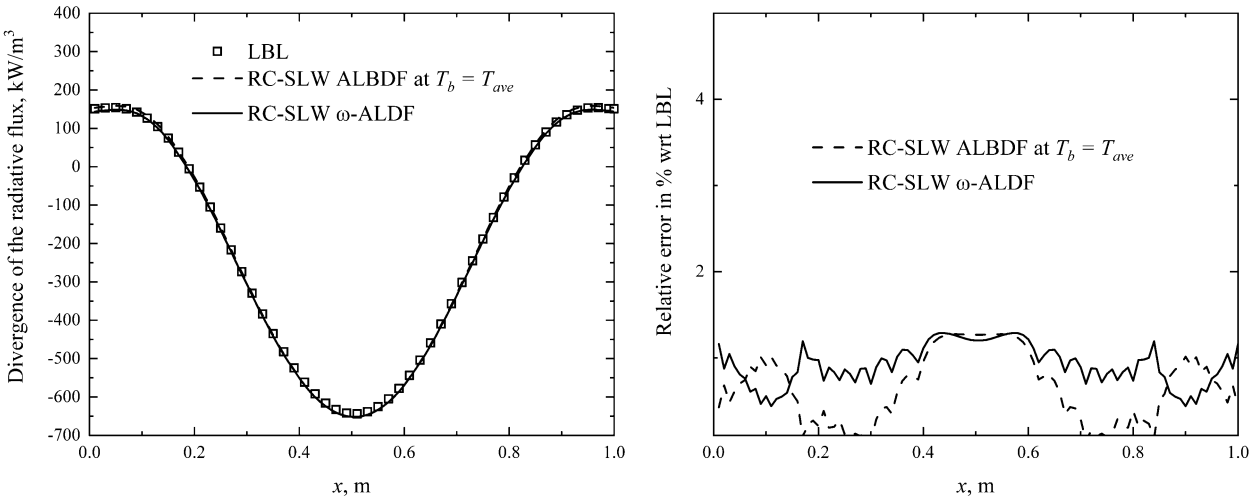

252

253 **Figure 2.** Single gas (H_2O) Case 2 (ΔT = 1500 K, ΔY_H = 0.2). Left: divergence of the radiative
254 flux. Right: relative error with respect to reference LBL calculations.

255 The predictions of Case 2 reveal that the accuracy of RC-SLW models based on both the ALBDF and
256 the ω-ALDF remains very high, with local errors that do not exceed 1.2%. Both RC-SLW methods
257 provide comparable levels of accuracy.

258 Figure 3 depicts a comparison of the weighting functions used in the conventional RC-SLW
259 model (the Planck functions averaged over 25 cm^{-1} narrow bands divided by the total Planck emission
260 at the average temperature of the gas defined in Eq. (16)) and the ω functions (averaged over the same
261 narrow band intervals) for Cases 1 and 2. One can notice that the weighting functions related to the
262 ALBDFs at the average temperature of the gas are the same for Cases 1 and 2, due to the definition
263 of this temperature Eq. (17).

264 The ω functions shown in Fig. 3, which are defined as volume averages of ratio of spectral / global
265 Planck functions, have a bell shape that first grows for small values of wavenumbers, reaches a
266 maximum and then decreases. In the two cases considered here, the maximum in $\omega(\eta)$ is attained for
267 wavenumbers lower than that of the maximum in the ALBDF weighting function evaluated at
268 $T_b = T_{ave}$. This suggests that the use of the ω-ALDF spectral distribution tends to increase the weights
269 at lower wavenumbers (related to low temperatures) as compared to the ALBDF spectral distribution.

This may explain why, in both Cases 1 and 2 (although the effect is more noticeable in Case 1), the accuracy of the RC-SLW model based on the ω-ALDF is higher near the walls, where the gas temperature is minimum.

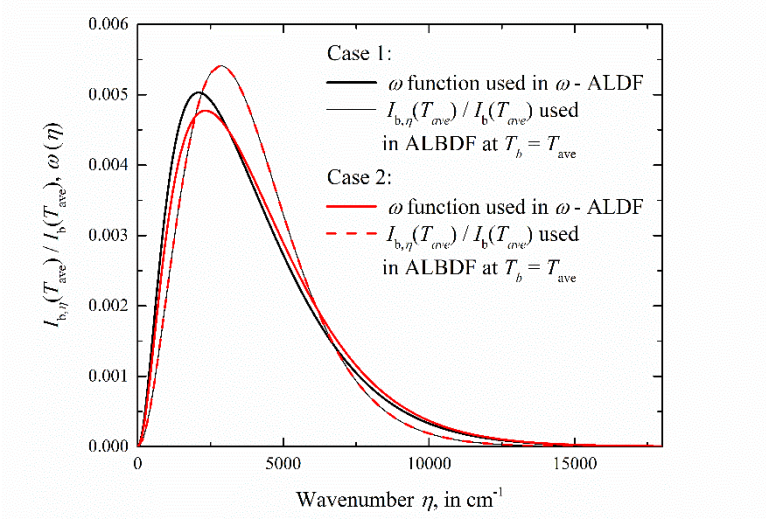

Figure 3. Comparison of (narrow band 25 cm^{-1} averaged) spectral weighting functions used to define the ALBDF / ω-ALDF.

Case 3 This case considers a mixture of absorbing species H_2O and CO_2 at atmospheric pressure. The temperature and species concentration profiles for this case are defined as:

$$T(x) = T_{\min} + \Delta T \sin(\pi x / L) \tag{21a}$$

$$Y_H(x) = Y_{H,\min} + \Delta Y_H \sin(\pi x / L) \tag{21b}$$

$$Y_C(x) = Y_H(x) / 2 \tag{21c}$$

For this case the following parameters were used: $\Delta T = 1000$ K, $T_{\min} = 500$ K, $Y_{H,\min} = 0.2$, and homogeneous mole fractions $\Delta Y_H = 0$ (and $\Delta Y_C = 0$). The properties of the gas mixture are treated by application of the multiplication approach, detailed in Refs. [Webb 2019, Solovjov 2018b]. Predictions are shown in Fig. 4.

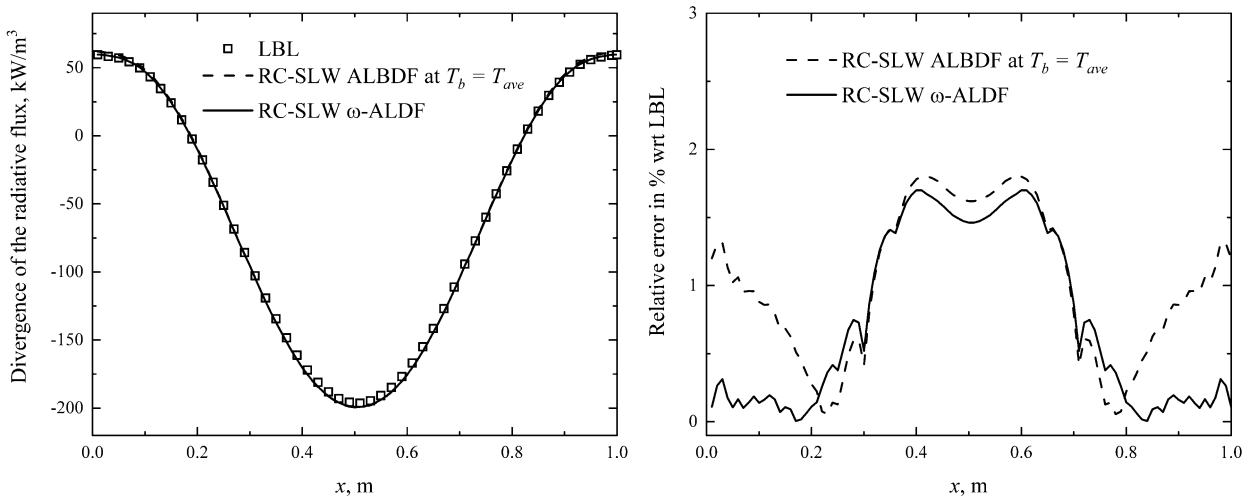

286

287 **Figure 4.** Gas mixture Case 3 (ΔT = 1000 K, ΔY_H = 0.0). Left: divergence of the radiative flux.
288 Right: relative error with respect to reference LBL calculations.

289 The results of Case 3 suggest that, as with Case 1 (which also considers a homogeneous layer), the
290 use of the ω-ALDF approach yields an accuracy higher near the walls than the ALBDF-based RC-
291 SLW model with blackbody source temperature specified as the volume-average temperature in the
292 domain. In the center of the layer, where the gas temperature reaches its maximum, the conventional
293 ALBDF RC-SLW method is somewhat more accurate than the RC-SLW method based on ω-ALDF.
294 However, this improved accuracy in the center of the profile does not fully compensate for the errors
295 near the walls. Globally, when averaged over the domain, the total errors related to the ω-ALDF are
296 smaller than the conventional RC-SLW method based on an ALBDF evaluated at the volume-
297 averaged temperature.

298 **Case 4** This case is identical to Case 3, but features a larger temperature difference (ΔT = 1500 K)
299 and includes spatial variation in species mole fractions, for $\Delta Y_H = 0.4$. The conditions of Case 4 are
300 representative of a confined, non-sooting pool fire situation. Results are presented in Fig. 5.

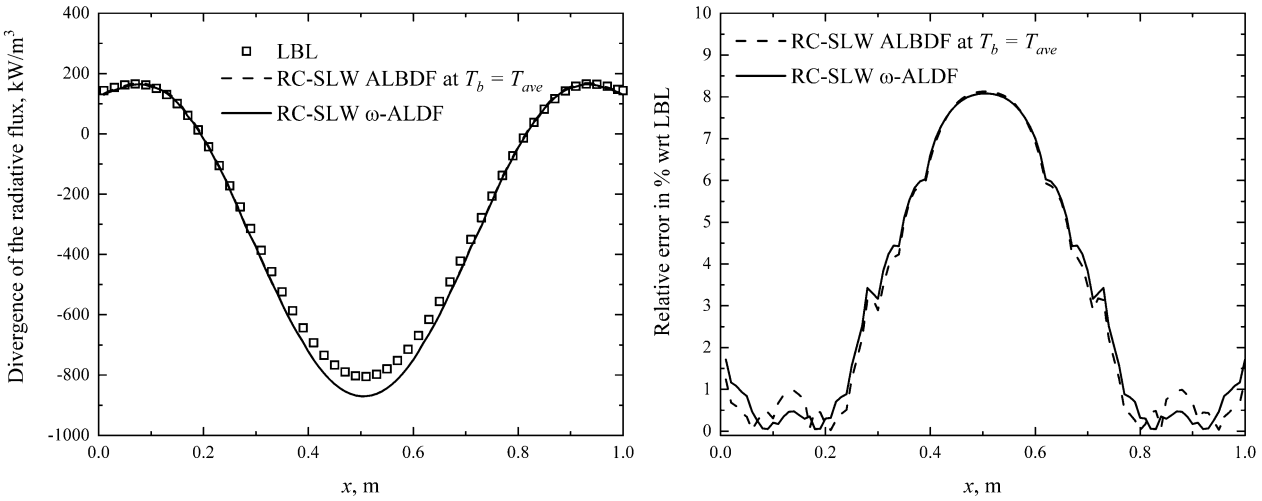

301

302 **Figure 5.** Gas mixture Case 4 (ΔT = 1500 K, ΔY_H = 0.4). Left: divergence of the radiative flux.
303 Right: relative error with respect to reference LBL calculations.

304 For Case 4, both the RC-SLW method based on the ALBDF (at $T_b = T_{ave}$) and the RC-SLW method
305 based on the ω-ALDF provide comparable local error, and neither of the two methods can be
306 reasonably considered as superior to the other. Both methods produce the highest error near the center
307 of the domain where the temperature is a maximum.

308 **Case 5** The fifth test case studied here was proposed recently by Wang [Wang 2021] and is presented
309 here to evaluate the ω-ALDF model in a case with three participating species. The layer is again one-
310 dimensional with spacing L = 0.1 m, and a mixture of three gas species H_2O, CO_2, and CO is
311 investigated. The temperature and species concentration profiles are given by the following
312 expressions:

313
$$T(x) = \begin{cases} 1500.0 \sin\left(\dfrac{5\pi}{3}\dfrac{x}{L} + \dfrac{\pi}{4}\right), & 0 \le x \le 0.3 \\ 6798.76 \exp\left(-7.3\dfrac{x}{L}\right), & 0.03 \le x \le L \end{cases} \tag{22a}$$

314
$$Y_H(x) = \begin{cases} 0.1 \sin\left(2\pi\dfrac{x}{L} + \dfrac{\pi}{4}\right), & 0 \le x \le 0.025 \\ 0.34 \exp\left(-6.28\dfrac{x}{L}\right), & 0.025 \le x \le L \end{cases} \tag{22b}$$

$$Y_C(x) = \begin{cases} 0.1 \sin\left(\dfrac{10\pi}{7}\dfrac{x}{L} + \dfrac{\pi}{4}\right), & 0 \le x \le 0.035 \\ 0.34 \exp\left(-4.49\dfrac{x}{L}\right), & 0.035 \le x \le L \end{cases} \tag{22c}$$

$$Y_{CO}(x) = \begin{cases} 0.02 \sin\left(\dfrac{10\pi}{3}\dfrac{x}{L} + \dfrac{\pi}{4}\right), & 0 \le x \le 0.015 \\ 0.068 \exp\left(-10.47\dfrac{x}{L}\right), & 0.015 \le x \le L \end{cases} \tag{22d}$$

Predictions for this case are shown in Fig. 6.

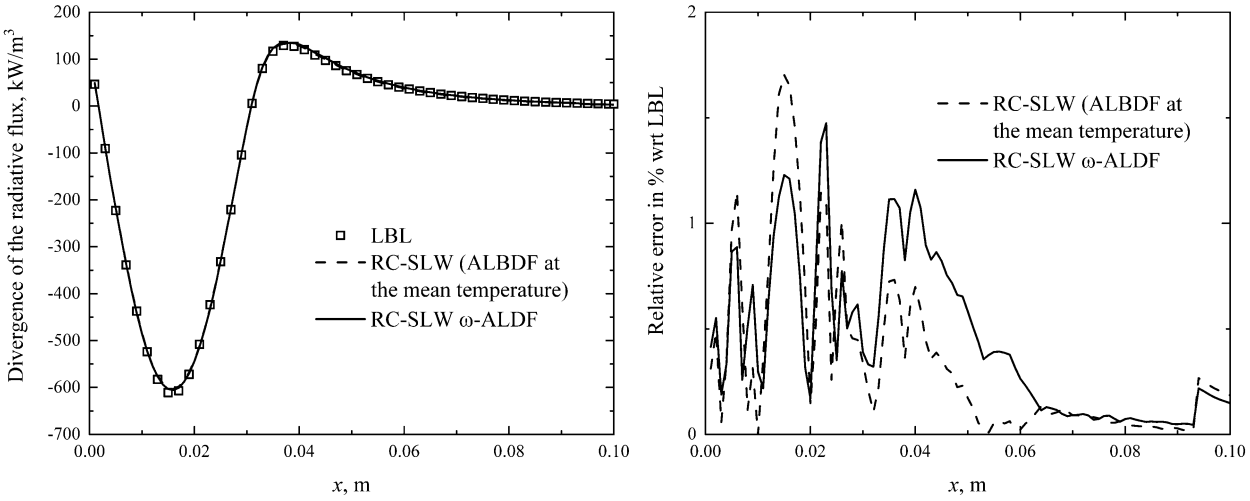

Figure 6. Gas mixture Case 5. Left: divergence of the radiative flux. Right: relative error with respect to reference LBL calculations.

Case 5 is the only scenario investigated in the present work with three absorbing molecules considered. As with the previous example cases, both RC-SLW models (based on ALBDF or ω-ALDF) provide a similar accuracy. The RC-SLW model based on the ALBDF at the average gas temperature appears to be slightly more accurate than the RC-SLW model based on ω-ALDF in the cold gaseous region (near $x = L$), but this gain cannot be considered significant enough to consider the ALBDF-based RC-SLW model to be more accurate, considering also that it yields modestly higher maximum error (slightly less than 2%) than the ω-ALDF model.

Case 6 The final case explored here considers a binary mixture of absorbing species H_2O and CO_2 but the gaseous medium is at a temperature lower than the walls. This case was selected because local

absorption by the gas is higher than its emission, whereas all previous cases considered are dominated by gaseous emission. The temperature and species concentration profiles for Case 6 are given as:

$$T(x) = 4500\left(x - 1/3\right)^2 + 500 \tag{23a}$$

$$Y_H(x) = 0.9\left(x - 1/3\right)^2 + 0.1 \tag{23b}$$

$$Y_C(x) = Y_H(x)/2 \tag{23c}$$

Results are shown in Fig. 7.

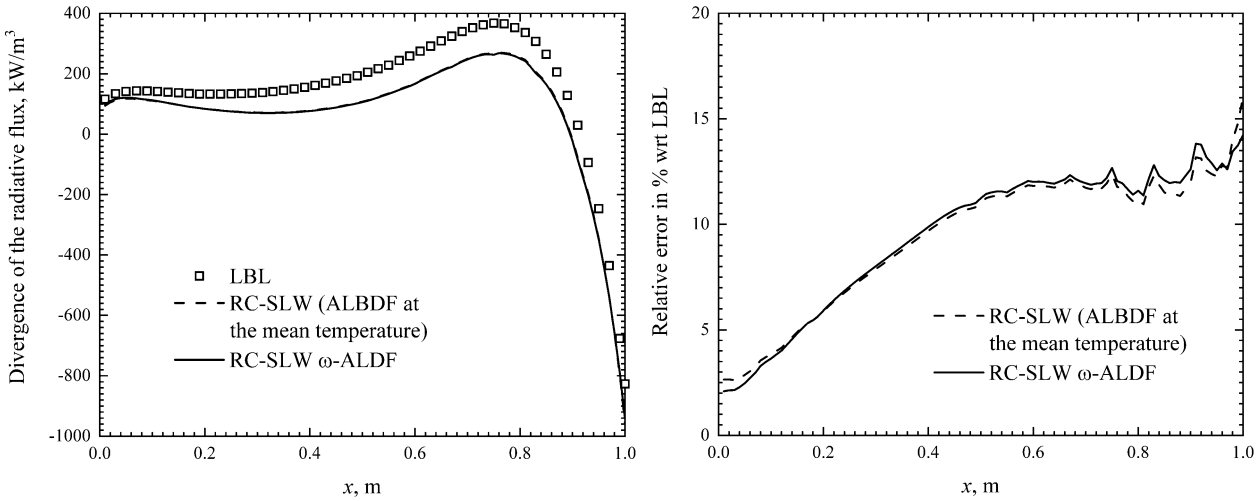

Figure 7. Gas mixture Case 6 in an absorption dominated case. Left: divergence of the radiative flux. Right: relative error with respect to reference LBL calculations.

The results presented in Fig. 7 reveal that, as in the previous cases, the results of both RC-SLW methods are similar. However, the accuracy of both methods in this absorption-dominated case is relatively poor for both the ω-ALDF and ALBDF based RC-SLW models. This can be explained by the fact that both methods are based on an averaging process over the gaseous volume. The ALBDF uses an average gas temperature and does not account for the possible influence of the emission-dominant boundaries; the ω-ALDF introduced here, *i.e.*, Eq. (14), is also founded on the gaseous volume only. This suggests that even if the concept of ω-ALDF permits the elimination of the possible dependence of the RC-SLW method on a rather arbitrary blackbody source temperature, it

does not in its present formulation allow treatment of all possible radiative transfer configurations with the same accuracy. One can notice that higher errors in absorption-dominated cases is not a deficiency unique to the ω-ALDF method: all SLW/FSK models provide similar errors in these types of scenarios. Further work is required to extend the present idea of ω-ALDF to absorption dominated scenarios.

Results of the various simulations (in terms of mean and maximum relative errors) considered in this work are summarized in Table 1. One can notice that even if mean relative errors are found to be similar in all simulations, the use of ω-ALDF is found to provide in most cases lower maximum errors.

CASE	Mean relative error (ALBDF/***ω-ALDF***)	Maximum relative error (ALBDF/***ω-ALDF***)
1	1.49 / ***1.03***	3.51 / ***1.56***
2	0.65 / ***0.92***	1.27 / ***1.29***
3	1.02 / ***0.74***	1.80 / ***1.70***
4	3.09 / ***3.15***	8.13 / ***8.08***
5	0.34 / ***0.44***	1.70 / ***1.47***
6	9.44 / ***9.56***	16.1 / ***14.3***

Table 1. Mean and maximum relative errors for the cases C1-6 considered in this work.

Finally, even if the objective of the paper was to show the feasibility of radiative transfer calculations without the need of any reference state and any blackbody source temperature through the combination of RC-SLW and ω-ALDF concepts, additional calculations were made to compare the technique with several standard methods that require these quantities as inputs. The first one is the original SLW model based on both a reference state and blackbody source temperature (the average

temperature was used here). This model, named RA for Reference Approach in the following, is equivalent to the FSCK-I model of Modest. The second one was proposed recently [Solovjov 2020] and is equivalent to Cai and Modest's improved FSCK (FSCK-II) method. All comparisons (only emission dominated cases already treated were recalculated) are made with 25 gray gases to comply with usual radiative transfer scenarios. Results are provided in Table 2 and Figures 8-10.

CASE	RC-SLW ALBDF	RC-SLW ω–ALDF	SLW RA	LC-SLW
1 (Figure 8)	1.47/*3.46*	1.02/*1.63*	1.70/*9.37*	3.23/*19.2*
2	0.69/*1.33*	0.93/*1.34*	0.96/*5.36*	2.30/*13.6*
3	1.03/*1.83*	0.76/*1.73*	1.02/*5.05*	1.52/*5.29*
4 (Figure 9)	3.14/*8.10*	3.19/*8.22*	2.99/*7.87*	4.01/*8.75*
5 (Figure 10)	0.33/*1.55*	0.44/*1.46*	0.07/*0.33*	0.30/*0.88*

Table 2. Mean / *Maximum* relative errors for the cases C1-5 with 25 gray gases.

From the values listed in Table 2, the following comments can be made:

- The LC-SLW / Cai and Modest's improved FSCK method is globally the less accurate model, providing the highest errors in four out of five cases. In three of these cases (C1-3), errors are at least two times higher than those of the RC-SLW / ω-ALDF combination.
- The SLW RA / FSCK-I method has the highest accuracy in Cases 4 and 5 (even if in Case 4 the order of magnitude is similar to the RC-SLW methods, or more precisely too close to these models to conclude reasonably that it is better than them). For Case 5, the level of accuracy observed with SLW RA / FSCK-I seems more fortuitous than a general property of the model.
- The RC-SLW methods perform equivalently well in Cases 1-3. Errors with 25 gray gases are higher than with 128 gray gases as shown in Table 1, but the general trend is the same. In four out of five cases, the use of ω-ALDF with RC-SLW provides a mean relative error lower or equal to 1%. In the

only case for which its mean relative error is higher than 1% (Case 4), it provides an accuracy on par all other methods.

Consequently, these calculations show that, in the cases considered, the RC-SLW model combined with the ω-ALDF concept provides an accuracy comparable with other existing methods (if we except case C5, for which the high accuracy of SLW RA / FSCK-I seems more due to chance than anything else). The RC-SLW / ω-ALDF combination can be safely recommended for radiative transfer calculation, since its accuracy is similar to other methods without any need to specify any rather arbitrary quantity, i.e., any reference state and blackbody source temperature as required by all other existing methods. The specification of these reference quantities does not appear to provide any improvement to global methods, which is in accordance with theory (see [André, 2017], where it was shown that no one of them is in fact required to construct a full spectrum gas radiation model).

Notice that for the cases considered here (1D geometries), the computational time required to evaluate the ω-ALDF was found to be negligible compared to the time required to read the look-up tables, solve the RTE, etc. 3D configuration will be treated as an extension of the present work to evaluate the cost of the method in more realistic and challenging situations.

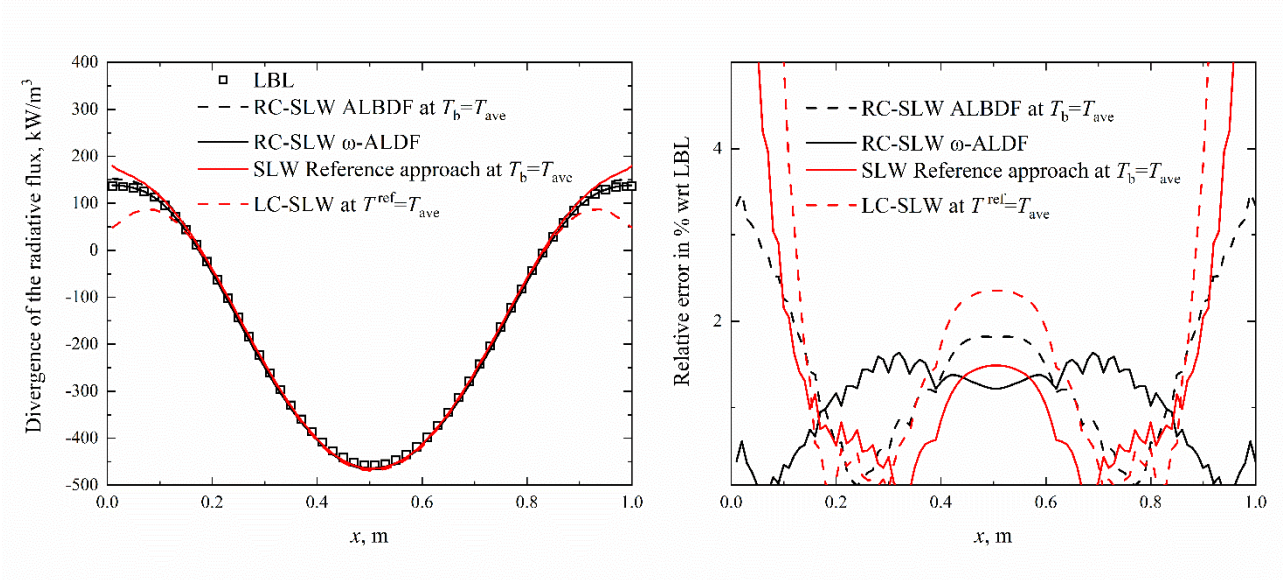

Figure 8. Single gas (H_2O) Case 1 (ΔT = 1500 K, ΔY_H = 0.0). Left: divergence of the radiative flux. Right: relative error with respect to reference LBL calculations. Calculations made with 25 gray gases.

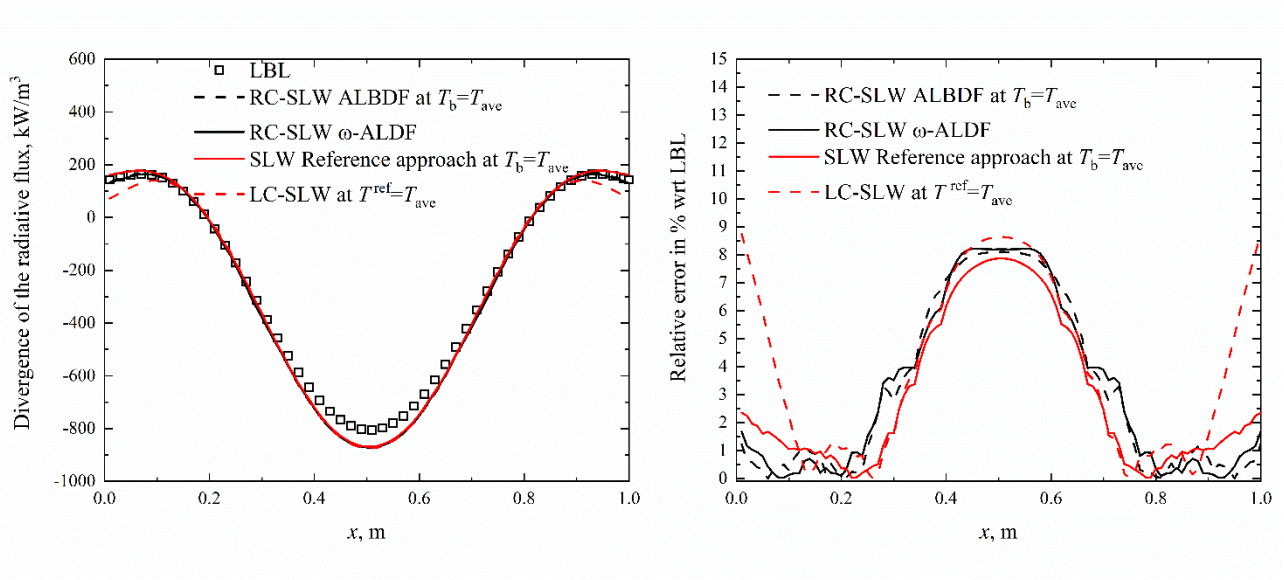

Figure 9. Gas mixture Case 4 (ΔT = 1500 K, ΔY_H = 0.4). Left: divergence of the radiative flux. Right: relative error with respect to reference LBL calculations. Calculations made with 25 gray gases.

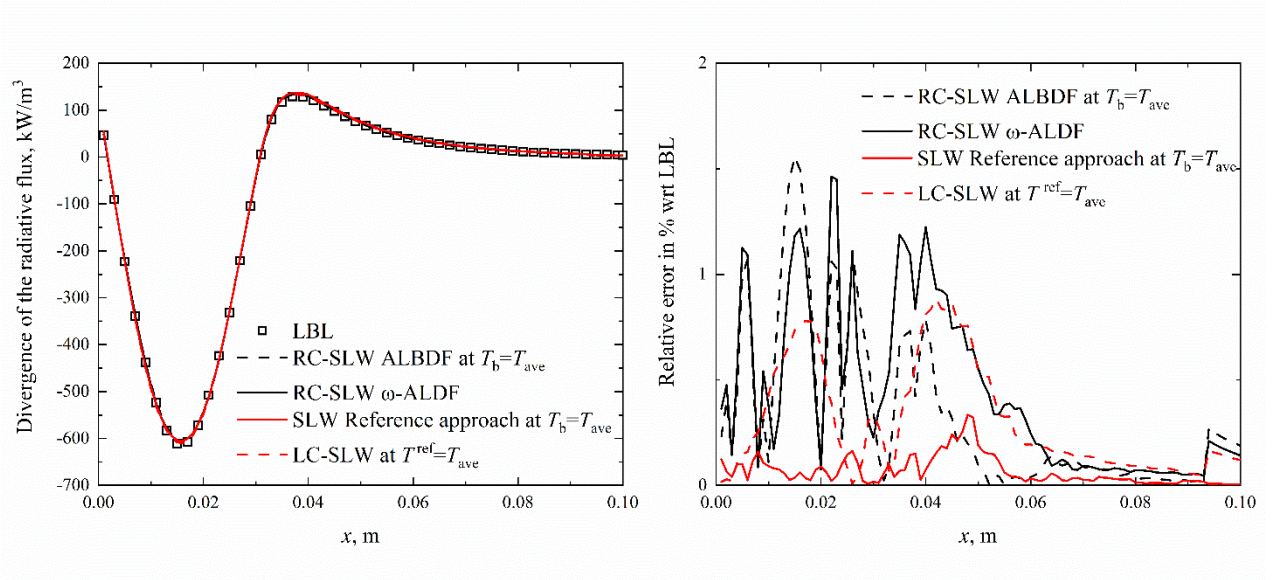

Figure 10. Gas mixture Case 5. Left: divergence of the radiative flux. Right: relative error with respect to reference LBL calculations. Calculations made with 25 gray gases.

CONCLUSIONS

The concept of a new spectral distribution function, termed the ω-ALDF, has been introduced as a generalization of the traditional ALBDF used in all variants of the SLW model. When combined with the RC-SLW/RC-FSK methods, the ω-ALDF model allows the construction of a full spectrum radiation transfer prediction method which is independent of any specified *à priori* quantity required by all other existing global methods. Thus, no user-specified parameter (*i.e.*, no reference temperature/concentration and no blackbody source temperature) is required for the solution. The proof-of-concept was verified on several test cases where predictions using the ω-ALDF model are compared to rigorous line-by-line benchmarks. In addition to demonstrating the concept, it was observed for all test cases that the accuracy of the modelling approach was either equivalent to or superior to the conventional ALBDF based RC-SLW method based on a blackbody source temperature defined as the volume-averaged temperature, as is usually recommended.

REFERENCES

André, F., Vaillon, R., Galizzi, C., Guo, H., Gicquel, O. [2011] A multispectral reordering technique for the full spectrum SLMB modeling of radiative transfer in non-uniform gaseous mixtures, *J. Quant. Spectr. Rad. Transfer*, Vol. 112, pp 394-411.

André, F., Solovjov, V.P., Webb, B.W., Lemonnier, D. [2017] Co-monotonic global spectral models of gas radiation in non-uniform media based on arbitrary probability measure, *J. Appl. Math. Modeling*, Vol. 50, pp 741-754.

Denison, M.K., Webb, B.W. [1993] Spectral line-based weighted-sum-of-gray-gases model for arbitrary RTE solvers, *ASME J. Heat Transfer*, Vol. 115, pp. 1004-1012.

Galtier, M., Roger, M., André, F., Delmas, A. [2017] A symbolic approach for the identification of radiative properties, *J. Quant. Spectr. Rad. Transfer*, Vol. 196, pp 130-141.

Maurente, A., Bruno, A.B., França, F.H.R., Howell, J.R. [2017] Non-dimensional wavenumber in full-spectrum *k*-distribution computations with or without a reference state, *J. Quant. Spectr. Rad. Transfer*, Vol. 196, pp. 222-229.

Modest, M. [2003] *Radiative Transfer*, 2nd Ed., Academic Press, New York.

Nelsen, R. B. [2007] *An Introduction to Copula*, Springer Science and Business Media.

Pearson, J.T., Webb, B.W., Solovjov, V.P. [2014] Effect of total pressure on the absorption line blackbody distribution function and radiative transfer in H_2O, CO_2 and CO, *J. Quant. Spectr. Rad. Transfer*, Vol. 143, pp 100-110.

Pierrot, L., Soufiani, A., Taine, J. [1999] Accuracy of narrow-band and global models for radiative transfer in H_2O, CO_2, and H_2O-CO_2 mixtures at high temperature, *J. Quant. Spectr. Rad. Transfer*. Vol. 62, pp. 523-548.

Roger, M., Maanane, Y., Galtier, M., André, F., Delmas, A. [2019] Symbolic Monte Carlo method based on orthogonal polynomial series: application to the phase function, in: Proceedings of the International Symposium on Radiative Transfer, RAD-19.

Solovjov, V.P. and Webb, B.W. [2008] Multilayer modelling of radiative transfer by SLW and CW methods in non-isothermal gaseous media, *J. Quant. Spectr. Rad. Transfer*, Vol. 109, pp 245-257.

Solovjov, V.P., Webb, B.W., André F. [2017] The rank correlated SLW model of gas radiation in non-uniform media, *J. Quant. Spectr. Rad. Transfer*, Vol. 197, pp 26-44.

Solovjov, V.P., Webb, B.W., André F. [2018a] The rank correlated FSK model for prediction of gas radiation in non-uniform media, and its relationship to the rank correlated SLW model, *J. Quant. Spectr. Rad. Transfer*, Vol. 214, pp 120-132.

Solovjov, V.P., Webb, B.W., André F. [2018b] *Radiative Properties of Gases*, in: F.A. Kulacki (Ed.) Handbook of Thermal Science and Engineering, Vol. 2, Springer, New York.

Solovjov, V.P., Webb, B.W., André, F., Lemonnier, D. [2020] Locally correlated SLW model for prediction of gas radiation in non-uniform media and its relationship to other global methods, *J. Quant. Spectr. Rad. Transfer*, Vol. 245(676):106857.

Young, S.J. [2013] *Band Model Theory of Radiation Transport*, The Aerospace Press.

Wang, C., Modest, M.F., Ren, T. Cai, J. He, B. [2021] Comparison and refinement of the various full-spectrum *k*-distribution and Spectral-Line-Based-Weighted-Sum-of-Gray-Gases Models for Nonhomogeneous Media, *J. Quant. Spectr. Rad. Transfer*, https://doi.org/10.1016.j.jqsrt.2021.107695.

Webb B.W., Solovjov V.P., André F. [2019] The spectral line weighted-sum-of-gray-gases (SLW) model for prediction of radiative transfer in molecular gases, *Adv. Heat Transfer*, Vol. 51, pp 207-298.

Appendix A. Justification of Eq. (6)

We provide here a justification rather than a rigorous proof of Eq. (6). Here, it is assumed that one can apply over the full spectrum the same assumptions on spectral lines as over narrow bands. In other words, the following assumptions are made [Young 2013]:

Assumption 1: The spectrum is composed of many (close to infinity) spectral lines randomly (and uniformly) spread over the wavenumber axis. For simplification purpose, the wavenumber axis is restricted to a bounded interval $\left[0,\eta^*\left(\varepsilon\right)\right]$. The upper limit $\eta^*\left(\varepsilon\right)$ is defined as follows. For any positive real $\varepsilon \approx 0$ and any temperature $T\left(dV\right),\ dV \in V$, one can define a wavenumber $\eta\left(\varepsilon, dV\right)$ such that

$$\int_0^{\eta(\varepsilon,dV)} \frac{I_{b\eta}\left[T\left(dV\right)\right]}{I_b\left[T\left(dV\right)\right]}\, d\eta = 1-\varepsilon \tag{A.1}$$

Considering the set of values of $\eta\left(\varepsilon, dV\right)$ obtained by using all the temperatures inside the computational domain, one can construct a sequence of intervals $\left[0,\eta\left(\varepsilon,dV\right)\right]$. There exists one temperature and an elementary volume dV^* in the domain such that for any $T\left(dV\right),\ dV \in V$, $\left[0,\eta\left(\varepsilon,dV\right)\right] \subset \left[0,\eta\left(\varepsilon,dV^*\right)=\eta^*\left(\varepsilon\right)\right]$. In this case, for all temperatures inside the domain, one has

$$\int_0^{\eta^*(\varepsilon)} \frac{I_{b\eta}\left[T\left(dV\right)\right]}{I_b\left[T\left(dV\right)\right]}\, d\eta \geq 1-\varepsilon \tag{A.2}$$

This method is used to define the upper limit $\eta^*\left(\varepsilon\right)$ used in Eq. (6).

Assumption 2: Linestrengths and positions are statistically independent.

Assumption 3: Line profiles are totally contained in spectral intervals over which the Planck function can be considered as constant.

From Assumption 1, the spectral absorption cross-section is the sum of the contribution of *N* spectral lines. Each spectral line has a linestrength S_n, a line center η_n and a profile f_n. The Planck mean absorption cross-section is:

$$C_P(dV,T) = \int_0^{+\infty} C_\eta\left[Y(dV),T(dV)\right]\frac{I_{b\eta}(T)}{I_b(T)}\,d\eta = \sum_{n=1}^{N}\left\{\int_0^{+\infty} C_{\eta,n}\left[Y(dV),T(dV)\right]\frac{I_{b\eta}(T)}{I_b(T)}\,d\eta\right\} \tag{A.3}$$

where $C_{\eta,n}$ is the spectral cross-section of the *n*-th spectral line. Its corresponding contribution to the total (for all spectral lines) Planck mean absorption cross-section is:

$$\int_0^{+\infty} C_{\eta,n}\left[Y(dV),T(dV)\right]\frac{I_{b\eta}\left[T(dV)\right]}{I_b\left[T(dV)\right]}\,d\eta = \int_0^{+\infty} S_n\left[T(dV)\right] f_n\left[\eta,\eta_n,Y(dV),T(dV)\right]\frac{I_{b\eta}\left[T(dV)\right]}{I_b\left[T(dV)\right]}\,d\eta \tag{A.4}$$

If one assumes that the line profile is fully contained inside a spectral interval over which the Planck function is constant (the value of the constant can then be taken equal to the value at the line center, consistent with Assumption 3), one has

$$\int_0^{+\infty} C_{\eta,n}\left[Y(dV),T(dV)\right]\frac{I_{b\eta}\left[T(dV)\right]}{I_b\left[T(dV)\right]}\,d\eta = S_n\left[T(dV)\right]\frac{I_{b\eta=\eta_n}\left[T(dV)\right]}{I_b\left[T(dV)\right]}\underbrace{\int_0^{+\infty} f_n\left[\eta,\eta_n,Y(dV),T(dV)\right]d\eta}_{=1} = S_n\left[T(dV)\right]\frac{I_{b\eta=\eta_n}\left[T(dV)\right]}{I_b\left[T(dV)\right]} \tag{A.5}$$

From this relationship one can rewrite the left-hand side of Eq. (6) as:

$$\int_0^{+\infty}\left\{C_\eta\left[Y(dV),T(dV)\right]-\bar{C}_\eta\right\}\frac{I_{b\eta}\left[T(dV)\right]}{I_b\left[T(dV)\right]}\,d\eta \approx \sum_{n=1}^{N}\left\{S_n\left[T(dV)\right]-\bar{S}_n\right\}\frac{I_{b\eta=\eta_n}\left[T(dV)\right]}{I_b\left[T(dV)\right]} \approx N\left[\frac{1}{N}\sum_{n=1}^{N}\left\{S_n\left[T(dV)\right]-\bar{S}_n\right\}\frac{I_{b\eta=\eta_n}\left[T(dV)\right]}{I_b\left[T(dV)\right]}\right] \tag{A.6}$$

where $\bar{S}_n$ is the volume average value of the linestrength of the *n*-th spectral line. From Assumption 2 (linestrengths and positions are statistically independent), the sum can be written as the product (as is done for mixtures of distinct gaseous species for instance):

521 $$\underbrace{\frac{1}{N}\sum_{n=1}^{N}\left\{S_n\left[T(dV)\right]-\bar{S}_n\right\}\frac{I_{b\eta=\eta_n}\left[T(dV)\right]}{I_b\left[T(dV)\right]}}_{\text{mean value of a function of both } S \text{ and } \eta}\approx\underbrace{\frac{1}{N}\sum_{n=1}^{N}\left\{S_n\left[T(dV)\right]-\bar{S}_n\right\}}_{\text{mean value of a function of } S \text{ only}}\underbrace{\frac{1}{N}\sum_{n=1}^{N}\frac{I_{b\eta=\eta_n}\left[T(dV)\right]}{I_b\left[T(dV)\right]}}_{\text{mean value of a function of } \eta \text{ only}} \quad \text{(A.7)}$$

522 And, from Assumption 1 (for *N* approaching infinity):

523 $$\frac{\eta^*(\varepsilon)}{N}\sum_{n=1}^{N}\frac{I_{b\eta=\eta_n}\left[T(dV)\right]}{I_b\left[T(dV)\right]}\approx\lim_{N\to+\infty}\frac{\eta^*(\varepsilon)}{N}\sum_{n=1}^{N}\frac{I_{b\eta=\eta_n}\left[T(dV)\right]}{I_b\left[T(dV)\right]}=\int_0^{\eta^*(\varepsilon)}\frac{I_{b\eta}\left[T(dV)\right]}{I_b\left[T(dV)\right]}\,d\eta\approx 1 \quad \text{(A.8)}$$

524 It then suffices to notice that (as line profiles are normalized):

525 $$\int_0^{+\infty}\left\{C_\eta\left[Y(dV),T(dV)\right]-\bar{C}_\eta\right\}d\eta=\sum_{n=1}^{N}\left\{S_n\left[T(dV)\right]-\bar{S}_n\right\} \quad \text{(A.9)}$$

526 to obtain Eq. (6).

527 One can notice that even if the set of assumptions required to derive the previous equation may
528 appear at first sight unreasonable, they are justified *á posteriori* by the accuracy of predictions based
529 on the ω-ALDF method as demonstrated in the paper. Furthermore, the approach used in the
530 Reference Approach SLW (RA-SLW), Absorption Distribution Function (ADF), and Full Scale
531 Correlated-*k* (FSCK) methods [Denison 1993, Pierrot 1999, Modest 2003] can be shown to be a
532 particular case of the assumption embodied in Eq. (6). This is detailed below for the FSCK method.

533 The total emission radiated by the volume *V* of gas can be written in terms of *f* as:

534 $$\int_V Y(dV)\,C_P\left[dV,T(dV)\right]I_b\left[T(dV)\right]dV=\bar{Y}\int_0^{+\infty}f(T)\,C_P\left[V(T),T\right]I_b(T)\,dT \quad \text{(A.10)}$$

535 where $C_P\left[V(T),T\right]$ is the Planck mean absorption cross-section at any location inside the volume
536 $V(T)$ occupied by the gas molecules at temperature *T*. This Planck mean is a constant with respect
537 to the gas molar fraction and only depends on the temperature of the gas, following Assumption 3.
538 Calling *F* the cumulative distribution of *f*, one can rewrite the previous equation as:

539 $$\int_V Y(dV)\,C_P\left[dV,T(dV)\right]I_b\left[T(dV)\right]dV=\bar{Y}\int_0^1 C_P\left[dV(F),T(F)\right]I_b\left[T(F)\right]dF \quad \text{(A.11)}$$

If the distribution f is smooth enough so that a single quadrature point over [0,1] can be used to evaluate the integral on the right-hand side of Eq. (A.11), then, writing this single point quadrature abscissa as F_0:

$$\int_V Y(dV)\, C_P\left[dV, T(dV)\right] I_b\left[T(dV)\right] dV = \bar{Y}\, C_P\left[dV(F_0), T(F_0)\right] I_b\left[T(F_0)\right] \qquad \text{(A.12)}$$

The temperature $T(F_0)$ then plays the role of some reference blackbody source temperature. In this particular case, the formulation presented here thus reduces to that used traditionally, for example, in the FSCK method [Modest 2003]. This provides further justification for the assumption of Eq. (6). This is because in this particular case (using again a single point quadrature to evaluate the integral between 0 and 1 which appears below)

$$\omega(\eta) = \int_0^{+\infty} f(T)\, \frac{I_{b\eta}(T)}{I_b(T)}\, dT = \int_0^1 \frac{I_{b\eta}\left[T(F)\right]}{I_b\left[T(F)\right]}\, dF = \frac{I_{b\eta}\left[T(F_0)\right]}{I_b\left[T(F_0)\right]} \qquad \text{(A.13)}$$